

## Solid-state Stereochemistry of Nefopam Hydrochloride, a Benzoxazocine Analgesic Drug<sup>1</sup>

Robert Glaser\*

Department of Chemistry, Ben Gurion University of the Negev, Beersheva 84105, Israel

Gernot Frenking and Gilda H. Loew

Life Sciences Division, SRI International, Menlo Park, California 94025, U.S.A.

David Donnell

Riker Laboratories, Loughborough, Leicestershire LE11 1EP

Shmuel Cohen and Israel Agranat

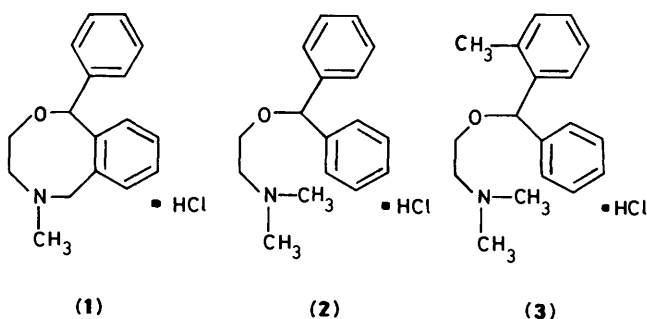
Department of Organic Chemistry, The Hebrew University of Jerusalem, Jerusalem 91904, Israel

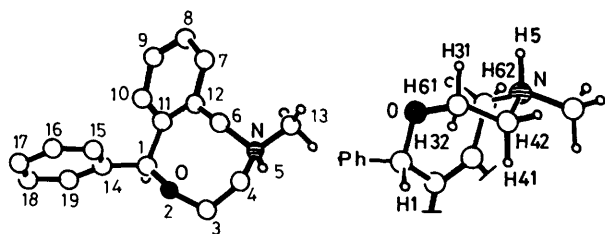
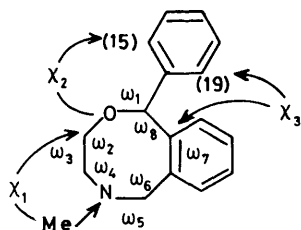
The solid-state structures of ( $\pm$ )- and (+)-nefopam hydrochloride (**1**), an analgesic agent, were determined by single-crystal X-ray diffraction analysis. ( $\pm$ )-Nefopam hydrochloride gave crystals belonging to the monoclinic  $P2_1/c$  space group, and at 298 K:  $a = 11.766(1)$ ,  $b = 7.741(1)$ ,  $c = 16.907(3)$  Å,  $\beta = 97.43(1)^\circ$ ,  $V = 1527.0(7)$  Å<sup>3</sup>,  $Z = 4$ ,  $R(F) = 0.0336$ , and  $R_w = 0.0452$ . (+)-Nefopam hydrochloride monohydrate gave crystals belonging to the orthorhombic  $P2_12_12_1$  space group, and at 298 K:  $a = 9.651(2)$ ,  $b = 19.747(2)$ ,  $c = 8.504(2)$  Å,  $V = 1620.7(7)$  Å<sup>3</sup>,  $Z = 4$ ,  $R(F) = 0.0432$ , and  $R_w = 0.0690$  for the (1*S*,5*S*)-model versus  $R(F) = 0.0442$ , and  $R_w = 0.0700$  for the (1*R*,5*R*)-model. The nefopam-HCl diastereoisomer found in the chiral crystal was also found in the racemic modification: (1*S*,5*S*) in (+)-(1)·H<sub>2</sub>O and (1*R*,5*R*), (1*S*,5*S*) in ( $\pm$ )-(1). The geometry of the nefopam-HCl molecule in both crystals is similar, and is that of a boat-(flattened chair) eight-membered ring. The *N*-methyl group is in an equatorial-like orientation, the oxydimethyleneamino moiety is in a *gauche* conformation, and the phenyl group resides in a relatively sterically unhindered *exo*-type position *trans* to the methyl. The major difference between the ( $\pm$ )-(1) and (+)-(1)·H<sub>2</sub>O molecular geometries is in the pitch of the phenyl ring. Energy minimization calculations on a series of nefopam-HCl boat-(flattened chair), twist-chair-(flattened chair), and twist-boat-(flattened chair) conformations were made by empirical force field methods using the MOLMEC molecular mechanics program. These calculations have shown that the (1*R*,5*R*), (1*S*,5*S*)-*exo*-phenyl-equatorial-methyl boat-(flattened chair) model for nefopam is the lowest energy structure in the series. Its geometry is analogous to that observed for crystalline ( $\pm$ )-(1) and (+)-(1)·H<sub>2</sub>O. This calculated molecular structure together with that of the axial *N*-methyl epimer correspond to the stereochemistry of the minor and major *N*-protonated solution species, respectively, upon dissolution of crystalline ( $\pm$ )-(1) or (+)-(1)·H<sub>2</sub>O in dichloromethane. The relatively small calculated energy difference (*ca.* 0.5 kcal mol<sup>-1</sup>) between the two epimers, which differ *via* diastereoisomerization through a prototropic shift/nitrogen inversion, is completely consistent with the magnitudes of the n.m.r. observed equilibrium ratios both in acidic aqueous medium or in dichloromethane solution (*ca.* 1:1 and *ca.* 3:2, respectively). The other calculated conformational models for nefopam-HCl geometry are not consistent with the n.m.r. data.

Racemic nefopam hydrochloride [( $\pm$ )-5-methyl-1-phenyl-3,4,5,6-tetrahydro-1*H*-2,5-benzoxazocine hydrochloride,<sup>2</sup> (**1**)] is an analgesic agent<sup>3,4</sup> which also exhibits some antidepressant activity.<sup>5</sup> It is a cyclized analogue of the parent antihistaminic diphenhydramine hydrochloride [( $\pm$ )-*NN*-dimethyl-2-(di-

phenylmethoxy)ethanamine hydrochloride<sup>6</sup> (**2**)], and is also related to orphenadrine hydrochloride [( $\pm$ )-*NN*-dimethyl-2-[(2-methylphenyl)phenylmethoxy]ethanamine hydrochloride<sup>7</sup> (**3**)], an anticholinergic agent with general muscle relaxant and antitremor properties used in the treatment of Parkinson's disease.<sup>8</sup> While nefopam hydrochloride is prescribed as the racemic modification ( $\pm$ )-(1), there are indications of different pharmacological potencies and metabolic behaviour for the two enantiomers [(+)-(1)·H<sub>2</sub>O and (-)-(1)·H<sub>2</sub>O].<sup>4,9-11</sup>

Recently, <sup>1</sup>H n.m.r. evidence has been presented showing that acidic aqueous solutions (pH or pD 1) of nefopam hydrochloride racemic modification ( $\pm$ )-(1) show two <sup>+</sup>NHCH<sub>3</sub> (or <sup>+</sup>NDCH<sub>3</sub>) diastereoisomeric species (*ca.* 1:1) differing in the stereochemistry of the *N*-methyl group.<sup>1</sup> <sup>1</sup>H and <sup>13</sup>C n.m.r. studies also indicate that two *N*-protonated diastereoisomeric species exist in unequal amounts (*ca.* 3:2) in dichloromethane or chloroform solutions of ( $\pm$ )-(1) or (+)-(1)·H<sub>2</sub>O.<sup>1</sup> The major and minor species were shown to have the *N*-methyl group disposed in an axial (**1a**) and equatorial (**1e**) type orientation, respectively.<sup>1</sup>



(1*S*, 5*S*)-(1*e*)Numbering diagram

Torsion angle diagram

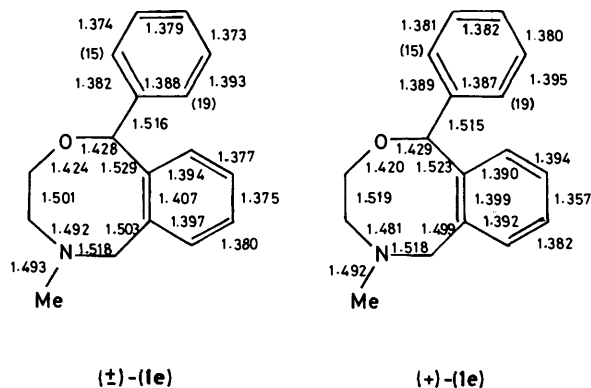
(±)-(1*e*)(+)-(1*e*)

Figure 1. Non-hydrogen bond distances (Å) for (±)-(1*e*) and (+)-(1*e*)·H<sub>2</sub>O, estimated standard deviation *ca.* 0.002 and *ca.* 0.003 Å, respectively

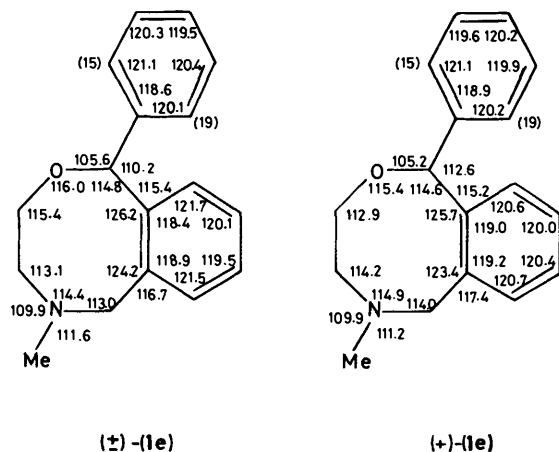
(±)-(1*e*)(+)-(1*e*)

Figure 2. Non-hydrogen bond angles (°) for (±)-(1*e*) and (+)-(1*e*)·H<sub>2</sub>O, estimated standard deviation *ca.* 0.2°

For the eight-membered ring nefopam hydrochloride (1) there exist a number of rationales for the n.m.r. observation of an equilibrium between equatorial and axial species in solution. In addition to conformational inhomogeneity, these include the prototropic shift *via* nitrogen inversion in the free base, and the ring-inversion pathways noted above. Preliminary evidence was recently presented pointing to a nefopam·HCl (1*e*,*a*) diastereoisomerization process involving a prototropic shift *via* inversion at the relatively labile chirotopic stereogenic<sup>12</sup> nitrogen.<sup>1</sup> Structurally constrained azacycles, such as tropane alkaloids (*e.g.* atropine·HBr, scopolamine·HBr, *etc.*) and cocaine·HCl, also readily undergo *N*-methyl epimerization in solution *via* the prototropic shift mechanism.<sup>13</sup> The presence of the ethano bridge in these cationic (8*r,s*)-8-methyl-8-azabicyclo[3.2.1]octane systems precludes diastereomerization in which equatorially oriented substituents are converted into axially disposed moieties *via* inversion of the chair conformation for the piperidine ring.<sup>13</sup>

This paper describes the stereochemical details of crystalline nefopam hydrochloride [(±)-(1) racemic modification, and chiral (+)-(1)·H<sub>2</sub>O] as determined by single-crystal X-ray diffraction. The crystal structure of (−)-nefopam hydrochloride monohydrate has been described while our studies were in progress.<sup>14</sup> Concurrent with our preliminary publication of the X-ray structures for the racemic modification and the (+)-enantiomer,<sup>1</sup> the structure of the racemate was also reported.<sup>15</sup> The brief description of (±)-(1) and (−)-(1)·H<sub>2</sub>O nefopam·HCl solid-state stereochemistry given by Klüfers *et al.*<sup>15</sup> and Hansen *et al.*<sup>14</sup> prompts us to report our conformational analysis of (1). In addition, empirical force field molecular mechanics calculations were performed to yield models for the non-crystallographically attainable axial *N*-methyl epimer (1*a*), as well as for conformational comparisons with crystalline equatorial *N*-methyl nefopam·HCl. These calculations were based on three benzoxazocine conformational archetypes and afforded twelve model structures (four diastereoisomers for each conformation). The calculated model of lowest energy (within the series) and X-ray-determined structures are very similar, and their molecular geometries are compared. It is shown that each of the two n.m.r.-observed solution species (1*a*,*e*) is consistent with the stereochemistry of only one calculated model structure.

## Results and Discussion

**Crystalline State Molecular Structures.**— The complete crystallographic details of the (±)-(1) and (+)-(1)·H<sub>2</sub>O crystals are listed in Table 1, and the fractional atomic co-ordinates of both molecular structures are listed in Tables 2 and 3. Non-hydrogen bond lengths, bond angles, and selected torsion angles are listed in Figures 1, 2 and Table 4, respectively.

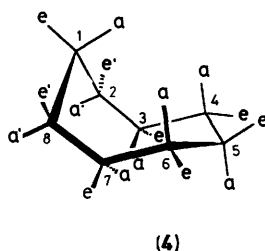
The nefopam·HCl diastereoisomer found in the chiral crystal was also found in the racemic modification: (1*S*,5*S*) in (+)-(1)·H<sub>2</sub>O and (1*R*,5*R*), (1*S*,5*S*) in (±)-(1). The powder diffraction of a sample of prescription grade (±)-(1) was found to be identical in all respects to that calculated from the single-crystal diffraction data. Recrystallization of the powder sample did not alter the solid-state configuration of the molecule. The finding of (1*S*,5*S*)-absolute configuration for (+)-(1)·H<sub>2</sub>O is consistent with the (1*R*)-configuration<sup>14</sup> described for the enantiomorph.

In both crystals the geometry of the nefopam·HCl molecule (1) is similar, and is that of a boat-chair<sup>16,17</sup> cyclo-octane severely flattened in the 'chair' region. This distortion from typical C<sub>s</sub> symmetry ideal boat-chair geometry results in the residence of the O(2) atom within very close proximity to the nearly planar region denoted by C(1), C(6), C(11), C(12) and the remaining benzo ring atoms. The *N*-methyl group is in an

**Table 1.** Crystallographic details for ( $\pm$ )-(1e) and (+)-(1e)·H<sub>2</sub>O

	( $\pm$ )-C <sub>17</sub> H <sub>19</sub> NO·HCl	(+)-C <sub>17</sub> H <sub>19</sub> NO·HCl·H <sub>2</sub> O
Formula weight	289.8	307.8
Space group	<i>P</i> 2 <sub>1</sub> / <i>c</i>	<i>P</i> 2 <sub>1</sub> 2 <sub>1</sub>
<i>a</i> (Å)	11.766(1)	9.651(2)
<i>b</i> (Å)	7.741(1)	19.747(2)
<i>c</i> (Å)	16.907(3)	8.504(2)
$\beta$ (°)	97.43(1)	
<i>V</i> /Å <sup>3</sup>	1 527.0(7)	1 620.7(7)
<i>Z</i>	4	4
$\rho_{\text{calc.}}$ /g cm <sup>-3</sup>	1.26	1.26
Linear abs. coeff. (cm <sup>-1</sup> )	2.03	1.98
<i>T</i> /K	298	298
Crystal size (mm <sup>3</sup> )	0.33 × 0.30 × 0.23	0.58 × 0.46 × 0.36
Radiation	graphite-monochromated Mo-K $\alpha$ ( $\lambda$ = 0.710 69 Å)	same
Collection range	$\pm h, k, l$	$+h, +k, +l$
2 $\theta$ limits	4.0 ≤ 2 $\theta$ ≤ 55.0°	same
Scan type	$\omega$ -2 $\theta$	same
Scan width (°)	0.80 + 0.35·tan $\theta$	same
Scan speed (° min <sup>-1</sup> )	1.27 to 4.12	same
Background time/scan time	0.33	same
Unique data	3 120	2 060
Unique data with $F_0^2 \geq 2\sigma(F_0^2)$	2 395	1 844
No. of variables	261	190
<i>R</i> ( <i>F</i> )	0.0336	0.0432 <sup>a</sup>
		0.0442 <sup>b</sup>
<i>R</i> <sub>w</sub> ( <i>F</i> )	0.0452	0.0690 <sup>a</sup>
		0.0700 <sup>b</sup>
Weighting factor <i>w</i>	$\sigma_F^{-2}$	$(\sigma_F^2 + 0.001\ 552 \cdot F^2)^{-1}$

<sup>a</sup> (1*S*,5*S*)-enantiomer model was used. <sup>b</sup> (1*R*,5*R*)-enantiomer model, obtained by reversing the sign of all atomic co-ordinates, was utilized.



equatorial-like orientation (e) that is *gauche* to the two diastereotopic protons on C(4) [henceforth, e will be affixed to both ( $\pm$ )-(1) and (+)-(1)·H<sub>2</sub>O crystal descriptors]. The oxydimethyleneamino fragment of the ring comprises the 'boat' region, and is found in a *gauche* conformation. The phenyl group resides in a relatively sterically unhindered *exo*-type position *trans* to the methyl. The major difference between the ( $\pm$ )-(1e)·H<sub>2</sub>O molecular geometries is in the pitch of the phenyl ring, e.g. the root mean square (r.m.s.) difference of the four phenyl ring pitch torsion angles O(2)-C(1)-C(14)-C(15), C(19) and C(11)-C(1)-C(14)-C(15), C(19) is 33.5° (compared with an r.m.s. difference of 7.4° for the comparison of the two sets of eight octagonal ring torsion angles).

The designation of a ( $\pm$ )-(1e) boat-(flattened chair) conformation was made on the basis of the signs and magnitudes of the eight octagonal ring torsion angles compared with the corresponding values for various ideal cyclo-octane conformations<sup>17</sup> (e.g. boat-chair, twist-chair-chair, twist-boat-chair, etc.). The boat-chair conformation was found to give the closest correlation to that found in ( $\pm$ )-(1e). The 'boat' region of the boat-(flattened chair) ( $\pm$ )-(1e) conformation gave the best agreement of both sign and magnitude *vis-à-vis* the ideal torsion angles {O(2)-C(3)-C(4)-N(5), C(3)-C(4)-N(5)-C(6), and C(4)-N(5)-C(6)-C(12): 57.7(2), -59.3(2), -49.1(2)°, respectively [for the

(1*S*,5*S*)-enantiomer in ( $\pm$ )-(1e)] *versus* 65.0, -65.0, -44.7°, respectively (for the ideal boat-chair)<sup>17</sup>}. The adjacent angles on either side of this region agreed in sign, but showed larger deviations in magnitude from the ideal values {C(1)-O(2)-C(3)-C(4), C(11)-C(1)-O(2)-C(3), and N(5)-C(6)-C(12)-C(11): 63.8(2), -82.7(2), 79.1(2)°, respectively [for the (1*S*,5*S*)-enantiomer in ( $\pm$ )-(1e)] *versus* 44.7, -102.2, 102.2°, respectively (for the ideal boat-chair)<sup>17</sup>}. The remaining two torsion angles [C(1)-C(11)-C(12)-C(6) and O(2)-C(1)-C(11)-C(12)] are in the 'chair' region of the boat-chair conformation and include the two adjacent *sp*<sup>2</sup>-hybridized ring atoms [C(11) and C(12)]. These two angles are close to synperiplanarity {3.2(3), and -6.5(2)°, respectively [for the (1*S*,5*S*)-enantiomer in ( $\pm$ )-(1e)]} and can be compared to the two oppositely signed 65° values observed in the ideal boat-chair<sup>17</sup> structure. Thus, while the 'boat' region of crystalline ( $\pm$ )-(1e) appears to be quite similar to the ideal boat-chair geometry, what should be the 'chair' region was found to contain the synperiplanar torsion angle, and is quite flattened.

Anet has noted that no conformation of cyclo-octane is strain free.<sup>17</sup> Perusal of structure (4) depicting this important C<sub>s</sub>-symmetry boat-chair conformation for cyclo-octane shows the presence of transannular non-bonding interactions [H(1a)···H(4a), H(1a)···H(6a), and H(3a)···H(7a)].<sup>17</sup> In addition, the approximately antiperiplanar 102.2° C(2)-C(3)-C(4)-C(5) and -102.2° C(5)-C(6)-C(7)-C(8) torsion angles in (4) result in eclipsing interactions between vicinal protons [H(3e)···H(4e) and H(6e)···H(7e)].<sup>17</sup> In the boat-(flattened chair) conformation for nefopam·HCl in ( $\pm$ )-(1e) and (+)-(1e)·H<sub>2</sub>O, most of these steric interactions are either eliminated in their entirety or are attenuated in their intensity. The methylene entity in position 7 of structure (4) has been replaced by a non-protonated atom [O(2)] in ( $\pm$ )-(1e) or (+)-(1e)·H<sub>2</sub>O. As a result, the severe non-bonded axial-axial H(3a)···H(7a) interaction in (4) has now been converted into a more distant H(61)···O(2) transannular interaction involving an axial

**Table 2.** Fractional atomic co-ordinates for ( $\pm$ )-(1e)<sup>a</sup>

Atom	x	y	z
Cl	0.978 57(4)	-0.196 13(6)	0.863 23(3)
C(1)	0.598 7(1)	0.233 7(2)	0.816 7(1)
O(2)	0.668 07(9)	0.088 3(1)	0.802 62(7)
C(3)	0.762 1(2)	0.122 0(3)	0.759 7(1)
C(4)	0.852 6(2)	0.240 0(3)	0.800 5(1)
N(5)	0.903 6(1)	0.176 0(2)	0.880 55(9)
C(6)	0.818 0(2)	0.151 7(2)	0.939 5(1)
C(7)	0.769 3(2)	0.416 5(3)	1.009 4(1)
C(8)	0.705 6(2)	0.562 9(3)	1.019 1(1)
C(9)	0.612 7(2)	0.601 1(3)	0.964 0(1)
C(10)	0.583 4(2)	0.493 7(2)	0.899 7(1)
C(11)	0.645 4(1)	0.344 0(2)	0.888 7(1)
C(12)	0.741 5(1)	0.305 7(2)	0.944 5(1)
C(13)	1.000 6(2)	0.290 0(4)	0.913 5(2)
C(14)	0.482 5(1)	0.160 2(2)	0.828 1(1)
C(15)	0.472 8(2)	0.041 9(3)	0.888 1(1)
C(16)	0.368 4(2)	-0.026 9(3)	0.899 1(1)
C(17)	0.270 6(2)	0.021 8(3)	0.850 3(1)
C(18)	0.278 5(2)	0.138 7(3)	0.790 2(1)
C(19)	0.384 3(2)	0.208 0(2)	0.778 5(1)
H(1)	0.590(1)	0.305(2)	0.770(1)
H(31)	0.794(2)	0.015(3)	0.752(1)
H(32)	0.735(2)	0.169(2)	0.708(1)
H(41)	0.823(2)	0.352(2)	0.807(1)
H(42)	0.918(2)	0.247(2)	0.770(1)
H(5)	0.932(2)	0.066(3)	0.874(1)
H(61)	0.781(1)	0.053(3)	0.925(1)
H(62)	0.866(1)	0.129(2)	0.989(1)
H(7)	0.836(2)	0.387(3)	1.049(1)
H(8)	0.722(2)	0.638(3)	1.063(1)
H(9)	0.562(2)	0.697(3)	0.969(1)
H(10)	0.517(2)	0.517(3)	0.863(1)
H(131)	0.973(2)	0.404(3)	0.915(1)
H(132)	1.038(2)	0.242(3)	0.964(2)
H(133)	1.055(2)	0.280(3)	0.875(1)
H(15)	0.540(2)	0.008(3)	0.922(1)
H(16)	0.366(2)	-0.110(3)	0.939(1)
H(17)	0.197(2)	-0.026(3)	0.859(1)
H(18)	0.210(2)	0.174(3)	0.755(1)
H(19)	0.395(2)	0.283(3)	0.736(1)

<sup>a</sup> Standard deviation in parentheses.**Table 3.** Fractional atomic co-ordinates for (+)-(1e)·H<sub>2</sub>O<sup>a</sup>

Atom	x	y	z
Cl	0.220 70(8)	0.409 52(4)	1.015 4(1)
C(1)	0.410 6(3)	0.177 3(1)	0.781 8(3)
O(2)	0.398 6(2)	0.228 01(9)	0.900 9(2)
C(3)	0.518 6(4)	0.268 3(2)	0.925 1(4)
C(4)	0.540 9(3)	0.320 4(1)	0.796 0(3)
N(5)	0.415 6(2)	0.360 1(1)	0.755 8(3)
C(6)	0.297 4(3)	0.319 1(1)	0.686 3(4)
C(7)	0.327 6(3)	0.281 5(2)	0.411 3(3)
C(8)	0.366 5(4)	0.235 3(2)	0.297 5(3)
C(9)	0.423 8(4)	0.175 2(2)	0.339 2(4)
C(10)	0.440 2(3)	0.158 9(2)	0.497 6(4)
C(11)	0.397 8(3)	0.203 7(1)	0.614 1(3)
C(12)	0.342 7(3)	0.266 4(1)	0.570 3(3)
C(13)	0.453 9(4)	0.417 8(2)	0.651 4(4)
C(14)	0.300 6(3)	0.125 2(1)	0.821 3(3)
C(15)	0.167 7(3)	0.129 0(1)	0.759 4(3)
C(16)	0.066 5(3)	0.083 3(2)	0.802 8(4)
C(17)	0.097 5(3)	0.032 9(1)	0.910 2(4)
C(18)	0.229 0(4)	0.028 2(2)	0.973 2(4)
C(19)	0.330 9(3)	0.074 5(1)	0.928 7(4)
OW	0.191 1(4)	0.446 7(1)	0.379 1(3)
H(1)	0.504	0.155	0.791
H(31)	0.501	0.207	1.015
H(32)	0.613	0.233	0.927
H(41)	0.584	0.302	0.701
H(42)	0.602	0.354	0.839
H(5)	0.369	0.378	0.848
H(61)	0.246	0.305	0.779
H(62)	0.241	0.355	0.638
H(7)	0.256	0.325	0.375
H(8)	0.339	0.252	0.193
H(9)	0.468	0.141	0.255
H(10)	0.498	0.113	0.532
H(131)	0.490	0.397	0.558
H(132)	0.386	0.447	0.633
H(133)	0.519	0.447	0.710
H(15)	0.146	0.161	0.688
H(16)	-0.030	0.086	0.762
H(17)	0.026	0.002	0.951
H(18)	0.258	-0.019	0.999
H(19)	0.431	0.076	0.979

<sup>a</sup> Standard deviation in parentheses.

proton and a ring atom (see Figure 3). In ( $\pm$ )-(1e) and (+)·H<sub>2</sub>O, the magnitudes of the O(2)-C(1)-C(11)-C(12) torsion angles [-6.5(2) and -17.0(4)°, respectively] illustrate that the O(2) atom resides close to or within the nearly planar region denoted by C(1), C(6), C(11), C(12) (and the remaining benzo ring atoms). These approximately synperiplanar torsion angles result in moving the H(1) atom farther away from its transannular counterpart H(41) [H(1), H(41) correspond in (4) to H(1a), H(6a), respectively]. Moreover, a transannular interaction of the type H(1a)···H(4a) in (4) is absent in (1e) since an *sp*<sup>2</sup>-hybridized carbon now occupies ring position 4. Finally, both H(3e)···H(4e) and H(6e)···H(7e) eclipsing interactions in (4) are eliminated in (1e) due to the occupation of O(2) and *sp*<sup>2</sup>-hybridized-C(12) in positions 7 and 4, respectively. A very similar boat-(flattened chair) conformation may be found for the 2,6-methano bridged 3-benzazocine system in benzomorphans [e.g. (2*R*,3*S*,6*R*,11*S*)/(2*S*,3*R*,6*S*,11*R*)-3,11-dimethyl-2,6-methano-1,2,3,4,5,6-hexahydro-3-benzazocine hydrochloride (5),<sup>18</sup> an 8-deoxybenzomorphan] and for the A, C, E ring systems within morphine<sup>19</sup> alkaloids.

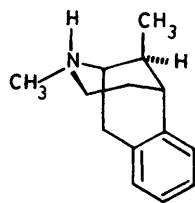
The X-ray crystallographically determined molecular structures of three cyclo-octane derivatives show boat-chair conformations containing an endocyclic synperiplanar torsion angle corresponding to C(6)-C(7)-C(8)-C(1) in (4): (1*R*,8*S*)/

(1*S*,8*R*)-9,9-dimethyl-9-azoniabicyclo[6.1.0]nonane iodide<sup>20</sup> ( $\pm$ )-(6), (1*R*,4*R*,8*S*)/(1*S*,4*S*,8*R*)-6,6,9,9-tetramethyl-3,5-dioxo-4-thiabicyclo[6.1.0]nonane 4-oxide<sup>21</sup> ( $\pm$ )-(7), and ( $\pm$ )-7-bromo-4-methyl-8,9-methylenedioxy-4',5',10-trimethoxy-1,2,5,6-tetrahydro-4*H*-3,4-benzoxazocine-2-spiro-1'-(1',3'-dihydro-3'-oxoisobenzofuran)<sup>22</sup> ( $\pm$ )-(8). These three boat-chair molecules have markedly less flattened 'chair' regions, and the synperiplanar torsion angles therein are located at the junction between 'chair' and 'boat' regions. These synperiplanar torsion angles in (6)-(8) occupy what is the smallest magnitude torsion angle in the C<sub>s</sub>-symmetry boat-chair conformation for cyclo-octane (4), and correspond in position to angle C(1)-O(2)-C(3)-C(4) in (1e). In conformation (4), torsion angles C(1)-C(2)-C(3)-C(4) and C(6)-C(7)-C(8)-C(1) are -44.7 and 44.7°, respectively (four other angles are ±65° and two are ±102.2°).<sup>17</sup> After benzo substitution at C(7,8) these torsion angles are transformed to -69 and 8.5°,<sup>22</sup> respectively, in (8). Inspection of Figure 3 shows that the severe H(3a)···H(7a) transannular interaction in (4) no longer exists in free amine (8), since an oxygen and an *sp*<sup>2</sup>-hybridized carbon now occupy positions 3 and 7, respectively. Both H(3e)···H(4e) and H(6e)···H(7e) eclipsing interactions in (4) are also eliminated in (8) via this very same replacement of methylene moieties at positions 3 and

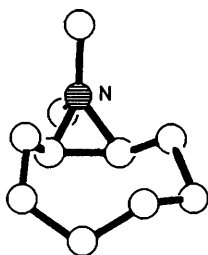
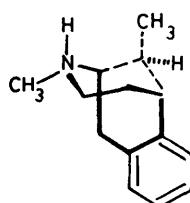
**Table 4.** Selected non-hydrogen torsion angles ( $^{\circ}$ ) for (1*S*,5*S*)-(±)-(1e), (1*S*,5*S*)-(+)-(1e)·H<sub>2</sub>O, and (12a,e)—(18a,e)

Structure	$\omega_1$	$\omega_2$	$\omega_3$	$\omega_4$	$\omega_5$	$\omega_6$	$\omega_7$	$\omega_8$	$\chi_1$	$\chi_2$	$\chi_3$
(±)-(1e) <sup>a</sup>	-82.7	63.8	57.7	-59.3	-49.1	79.1	3.2	-6.5	174.2	58.7	115.0
(+)-(1e) <sup>a</sup>	-78.1	74.9	48.0	-64.3	-41.0	79.3	4.7	-17.0	169.4	91.3	149.4
(12e) <sup>b</sup>	-77.0	63.9	59.8	-66.6	-43.9	80.5	2.9	-12.4	173.7	80.0	133.9
(18e) <sup>b</sup>	-79.5	61.8	60.5	-62.3	-48.2	79.4	2.8	-6.9	173.4	78.9	138.9
(12a) <sup>c</sup>	-73.3	68.0	53.4	-62.3	-46.4	84.6	2.3	-17.3	60.2	85.8	139.5
(18a) <sup>b</sup>	-73.2	69.0	51.7	-62.1	-45.8	83.4	2.0	-15.9	64.9	85.6	138.9
(13e) <sup>c</sup>	78.0	-64.9	-59.1	66.3	43.4	-82.0	-0.1	10.2	-174.0	100.8	148.9
(13a) <sup>b</sup>	75.7	-68.0	-53.8	61.6	46.9	-85.7	0.8	13.2	-60.9	97.5	146.0
(14e) <sup>c</sup>	-49.3	125.9	-79.6	53.0	-90.8	93.7	0.2	-31.1	173.3	-77.4	-25.5
(14a) <sup>b</sup>	-52.9	127.9	-77.1	47.0	-85.2	89.7	2.4	-29.3	-76.8	-80.0	-27.9
(15e) <sup>b</sup>	35.7	-121.0	83.2	-52.1	88.5	-96.0	-1.2	41.2	-172.5	66.0	115.5
(15a) <sup>c</sup>	44.9	-126.0	79.4	-46.0	83.1	-91.5	-2.0	34.7	77.8	76.7	126.7
(16e) <sup>c</sup>	-39.1	-67.8	107.5	-69.7	77.4	-86.5	1.5	84.8	170.8	-153.5	-97.7
(16a) <sup>b</sup>	-38.9	-68.3	105.6	-63.0	70.8	-84.1	0.6	85.8	61.3	-153.9	-98.2
(17e) <sup>b</sup>	15.8	87.4	-100.9	61.9	-82.1	93.1	0.8	-73.2	-178.5	165.2	-148.0
(17a) <sup>c</sup>	18.4	86.0	-100.4	56.2	-74.9	89.4	2.0	-75.2	67.8	166.0	-147.9

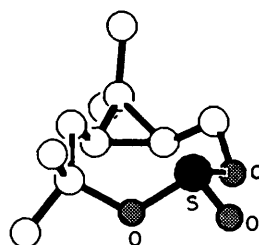
<sup>a</sup> Estimated standard deviation *ca.* 0.2° and *ca.* 0.3° for (1*S*,5*S*)-(±)-(1e), (1*S*,5*S*)-(+)-(1e)·H<sub>2</sub>O, respectively. In (±)-(1e) and (+)-(1e)·H<sub>2</sub>O the dihedral angles between the two aromatic planes are 85.0 and 89.5°, respectively. <sup>b</sup> (1*S*,5*S*)-Configuration. <sup>c</sup> (1*S*,5*R*)-Configuration.



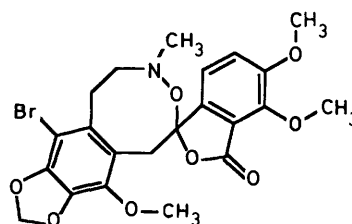
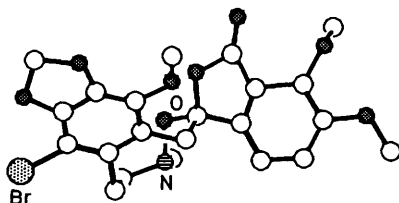
(5)



(6)



(7)



(8)

7. Hendrickson has calculated the excess of strain energy resulting from replacement of a proton by a methyl substituent at various positions on the *C<sub>s</sub>*-symmetry boat-chair cyclo-octane ring.<sup>23</sup> Only at carbon 2 in (4) were low values noted for methyl substitution at both of its two diastereotopic sites [0.5 kcal

mol<sup>-1</sup> for methyl in either the 2-equatorial or 2-axial position].<sup>23</sup> It is therefore not surprising that position 2 provides the spiro ring junction point in (8). Of the two transannular H(1a)···H(4a), H(1a)···H(6a) interactions noted in (4), only one [H(1a)···H(6a)] remains in (8) due to

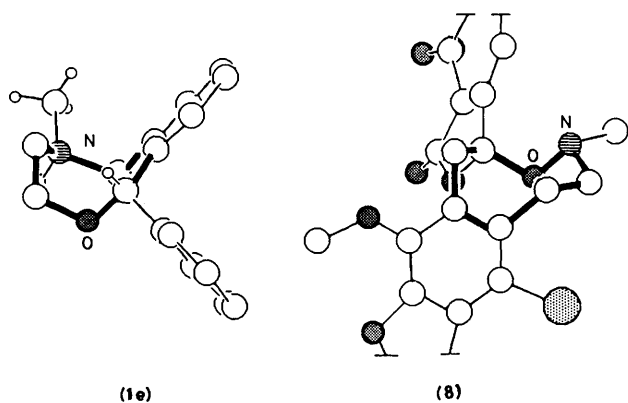
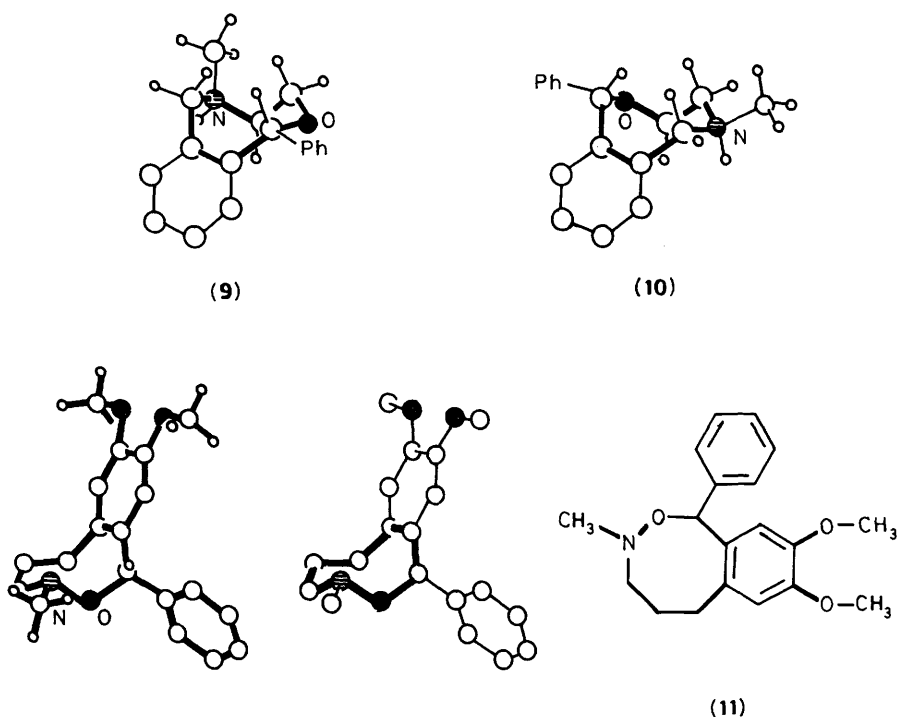


Figure 3. Comparison of the boat-(flattened chair) conformation for ( $\pm$ )-(1e) with the boat-chair conformation of ( $\pm$ )-(8)



the presence therein of an axial pair of non-bonding electrons attached to the free amino nitrogen at position 4. Finally, occupancy of the 4-equatorial site by the *N*-methyl group in (8) is consistent with the finding by Hendrickson<sup>23</sup> of an excess of strain energy of 0.5 kcal mol<sup>-1</sup> [compared with 5.1 kcal mol<sup>-1</sup> for substitution of H(4a) by methyl].

Two structures (9) and (10) may be drawn for nefopam hydrochloride bent into a boat-chair conformation in a manner similar to that found in (8) [*i.e.* a synperiplanar torsion angle of the type C(6)–C(7)–C(8)–C(1) seen in (4)]. Both structures would suffer from the same transannular H(1a)···H(4a), H(4a)···H(6a) interactions noted in (4), and both would show the H(3e)···H(4e) eclipsing interactions seen in (4). It is noted that these non-bonded interactions are missing in the experimentally observed boat-(flattened chair) conformation for (1e). The phenyl and methyl groups in (9) may occupy 6e and 2e' positions, respectively, on the boat-chair cyclo-octane ring for (4), while in (10) they can be located at 1e and 5e, respectively. These equatorial positions are all expected to be less sterically demanding than their axial counterparts.<sup>23</sup>

The boat-chair conformation is not the only one found by *X*-

ray crystallography for benzoxazocines. The one other benzoxazocine solid-state structure in the literature [( $\pm$ )-8,9-dimethoxy-3-methyl-1-phenyl-3,4,5,6-tetrahydro-1*H*-2,3-benzoxazocine<sup>24</sup> ( $\pm$ )-(11)] exists in the crystal in a conformation which can best be described as a twist-chair-chair<sup>17</sup> modified by two adjacent *sp*<sup>2</sup>-hybridized ring atoms.\* As in the case of the modified boat-chair in nefopam·HCl ( $\pm$ )-(1e), the greatest distortion from ideal (twist-chair-chair) geometry<sup>17</sup> is in the region containing the two adjacent *sp*<sup>2</sup>-hybridized ring atoms.\* As in the case of the boat-(flattened chair) conformation, this distortion results in a twist-chair-(flattened chair) structure.

Empirical force field calculations using the MOLMEC<sup>25</sup> molecular mechanics program were performed on nefopam·HCl molecules bent into one of three conformational types: boat-(flattened chair), twist-chair-(flattened chair), and twist-boat-(flattened chair). Four diastereoisomers were calculated for each conformation [(1) *exo*-phenyl, equatorial methyl; (2) *endo*-

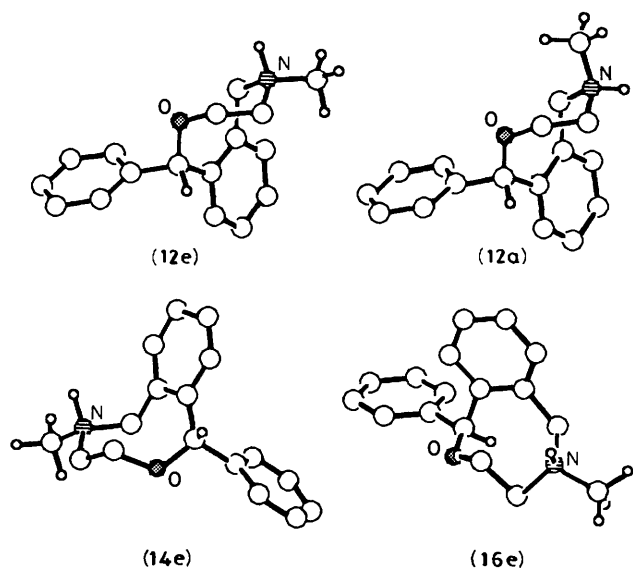
phenyl, axial methyl; (3) *exo*-phenyl, axial methyl; and (4) *endo*-phenyl, equatorial methyl]. The *X*-ray-determined octagonal ring torsion angles of ( $\pm$ )-(1e) and ( $\pm$ )-(11)<sup>24</sup> provided the starting parameters for the boat-(flattened chair) (12a,e)–

\* The torsion angles O(2)–N(3)–C(4)–C(5), N(3)–C(4)–C(5)–C(6), and C(4)–C(5)–C(6)–C(12) gave the best agreement of both sign and magnitude *vis-à-vis* the ideal values {–77.2(3), 53.9(4), –88.0(4)°, respectively [for (1*S*,3*R*)-enantiomer in ( $\pm$ )-(1), calculated from data in ref. 24], *versus* –82.4, 56.2, –82.4°, respectively (for ideal twist-chair-chair)<sup>18</sup>}. The adjacent angles on either side of this region agreed in sign, but showed larger deviations in magnitude from the ideal values {C(1)–O(2)–N(3)–C(4), C(11)–C(1)–O(2)–N(3), and C(5)–C(6)–C(12)–C(11): 134.0(2), –61.2(2), 80.8(4)°, respectively [for (1*S*,3*R*)-enantiomer in ( $\pm$ )-(11)], *versus* 114.6, –82.4, 114.6° respectively (for ideal twist-chair-chair)<sup>18</sup>}. The remaining two torsion angles include the two adjacent *sp*<sup>2</sup>-hybridized ring atoms [C(11) and C(12)], and are the smallest angles (one of which is close to synperiplanarity). These correspond to two oppositely signed ideal values {C(1)–C(11)–C(12)–C(6) and O(2)–C(1)–C(11)–C(12): 8.7(4), –29.5(3)°, respectively [for (1*S*,3*R*)-enantiomer in ( $\pm$ )-(11)], *versus* –82.4, 56.2°, respectively [for ideal (twist-chair-chair)<sup>18</sup>]}.

**Table 5.** Molecular mechanics calculated energies for diastereoisomers of nefopam [cations (12a,e)—(17a,e), and free base (18a,e)]<sup>a</sup>

Configuration	Ring conformation	1-Ph	N-Me	Energy <sup>b</sup>	Relative energy <sup>b</sup>
1 ( <i>RR,SS</i> )	Boat-(flattened chair) (12e)	<i>exo</i>	Equatorial	36.68	0.0
2 ( <i>RS,SR</i> )	Boat-(flattened chair) (12a)	<i>exo</i>	Axial	37.3	0.6
3 ( <i>RS,SR</i> )	Boat-(flattened chair) (13e)	<i>endo</i>	Equatorial	37.5	0.8
4 ( <i>RR,SS</i> )	Boat-(flattened chair) (13a)	<i>endo</i>	Axial	38.1	1.4
5 ( <i>RS,SR</i> )	Twist-chair-(flattened chair) (14e)	<i>exo</i>	Equatorial	36.73	0.05
6 ( <i>RR,SS</i> )	Twist-chair-(flattened chair) (14a)	<i>exo</i>	Axial	39.6	2.9
7 ( <i>RR,SS</i> )	Twist-chair-(flattened chair) (15e)	<i>endo</i>	Equatorial	38.7	2.0
8 ( <i>RS,SR</i> )	Twist-chair-(flattened chair) (15a)	<i>endo</i>	Axial	41.6	4.9
9 ( <i>RR,SS</i> )	Twist-boat-(flattened chair) (16e)	<i>endo</i>	Equatorial	38.5	1.8
10 ( <i>RS,SR</i> )	Twist-boat-(flattened chair) (16a)	<i>endo</i>	Axial	41.2	4.5
11 ( <i>RS,SR</i> )	Twist-boat-(flattened chair) (17e)	<i>exo</i>	Equatorial	39.0	2.3
12 ( <i>RR,SS</i> )	Twist-boat-(flattened chair) (17a)	<i>exo</i>	Axial	41.9	5.2
13 ( <i>RR,SS</i> )	Boat-(flattened chair) free base (18e)	<i>exo</i>	Equatorial	29.4	[0.6] <sup>c</sup>
14 ( <i>RS,SR</i> )	Boat-(flattened chair) free base (18a)	<i>exo</i>	Axial	28.8	[0.0] <sup>c</sup>

<sup>a</sup> Energy-minimized geometries calculated using the MOLMEC program.<sup>21</sup> <sup>b</sup> kcal mol<sup>-1</sup>. <sup>c</sup> Relative energy comparison between the two free-base diastereoisomers.



(13a,e) and twist-chair-(flattened chair) diastereoisomers (14a,e)—(15a,e). The starting parameters for the twist-boat-(flattened chair) octagonal ring [in diastereoisomers (16a,e)—(17a,e)] were produced during energy optimization on a twist-chair-(flattened chair) species. Two boat-(flattened chair) nefopam free-base diastereoisomers (18a,e) each having *exo*-phenyl substituents, but differing in the orientation of *N*-methyl group, were also calculated. The starting parameters for the free bases were obtained by replacement of a lone pair of electrons for the *NH* proton of the corresponding protonated amine. The selected torsion angles characterizing each of the fourteen calculated structures (12a,e)—(18a,e) are listed in Table 4. The calculated optimized energies for these fourteen species are listed in Table 5. Each of the four calculated boat-(flattened chair) (12a,e)—(13a,e) and (twist-chair) (14a,e)—(15a,e) diastereoisomers exhibited energy-minimized final octagonal ring torsional angles similar to those noted for crystalline (±)-(1e) and (±)-(11),<sup>25</sup> respectively. Of the 12 nefopam-HCl calculated geometries, the (1*R*,5*R*), (1*S*,5*S*)-*exo*-phenyl, equatorial-methyl boat-(flattened chair) model (12e) was the lowest-energy structure in the series, and all its bonding parameters were

found to be similar to those found for crystalline (±)-(1e) and (+)-(1e)·H<sub>2</sub>O. It is noted that while (12e) was found to be the lowest-energy structure of the twelve calculated nefopam-HCl models, a designation 'global minimum' may be slightly misleading since boat-(flattened chair) (12e) was only 0.05 kcal mol<sup>-1</sup> lower than twist-chair-(flattened chair) (14e).

In the 12 nefopam-HCl models, all the axial *N*-methyl group structures are higher in energy than their corresponding equatorial epimers (see Table 5). In the twist-chair-(flattened chair) (14a,e)—(15a,e) and twist-boat-(flattened chair) (16a,e)—(17a,e) structures, the energy difference between the two *N*-methyl diastereotopic equatorial, axial dispositions [e.g. (14e) versus (14a), 2.8 kcal mol<sup>-1</sup>] is greater than that seen between the two *exo,endo* 1-phenyl orientations [e.g. (14e) versus (15e), 1.9 kcal mol<sup>-1</sup>], while the situation is reversed in the set of boat-(flattened chair) diastereoisomers [e.g. (12e) versus (12a), 0.6 kcal mol<sup>-1</sup>; (12e) versus (13e), 0.8 kcal mol<sup>-1</sup>]. In all six equatorial *N*-methyl group models (12e)—(17e) no significant non-bonding interactions were noted involving that group. However, only in the boat-(flattened chair) isomers (12a) and (13a) was a similar situation found for the axial *N*-methyl group [severe non-bonded interactions were seen for axial *N*-methyl in (14a)—(17a)]. Similarly, no significant non-bonding interactions were noted for the *exo*-oriented phenyl group in boat-(flattened chair) (12e), while such interactions were observed for the higher energy *endo*-directed phenyl group boat-(flattened chair) diastereoisomers (13a,e). In the twist-chair-(flattened chair) and twist-boat-(flattened chair) conformations, non-bonding interactions were found for the phenyl group in either *exo*- or *endo*-orientation.

N.m.r. spectroscopic evidence suggests that a prototropic shift/nitrogen inversion mechanism is the diastereoisomerization process for solutions of nefopam hydrochloride (1),<sup>1</sup> as it is for the more constrained tropane alkaloids<sup>13</sup> and opiate agonists or antagonists.<sup>26–28</sup> The pH dependency for dynamic n.m.r. behaviour noted when crystalline (±)-(1e) [calc. (12e)], is dissolved in aqueous medium is in accord with the proposed prototropic shift/nitrogen inversion pathway (increasing the acidity of aqueous solutions increases the n.m.r. lifetimes of *N*-protonated species<sup>13,29</sup>).<sup>1</sup> Dissolution of the nefopam hydrochloride salt in dichloromethane solvent also increases the n.m.r. lifetimes of the *N*-protonated species.<sup>1,13</sup> As noted above, the (1*R*,5*S*), (1*S*,5*R*)-*exo*-phenyl, axial-methyl boat-(flattened chair) model (12a) was found to be slightly higher in energy (*ca.* 0.5 kcal mol<sup>-1</sup>) than the epimeric 'global

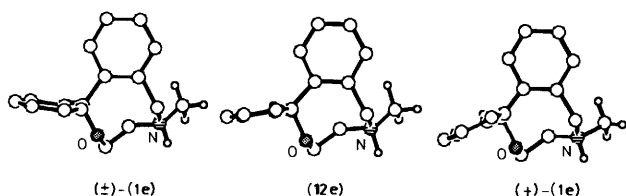
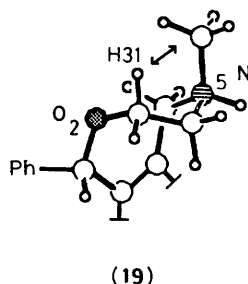


**Figure 4.** Comparison of the crystalline (1*S*,5*S*)-nefopam hydrochloride molecular conformations *versus* that of the calculated model (12*e*) in all drawings, the benzo ring resides in the plane of the paper



minimum' energy structure (1*R*,5*R*),(1*S*,5*S*)-*exo*-phenyl, equatorial methyl (12*e*). This relatively small calculated energy difference between the two diastereoisomers (12*e*,**a**), which can be interconverted *via* epimerization through a prototropic shift/nitrogen inversion, is completely consistent with the magnitudes of the experimentally observed equilibrium ratios in both acidic aqueous medium or dichloromethane solution [*ca.* 1:1 and *ca.* 3:2, respectively<sup>1</sup>]. Finally, the <sup>1</sup>H n.m.r. vicinal coupling constants recorded from solutions of (±)-(1*e*) or (+)-(1*e*)·H<sub>2</sub>O are in complete agreement *only* with a boat-(flattened chair) conformational geometry for each of the two species (12*a*,**e**).<sup>1</sup>

The two calculated boat-(flattened chair) nefopam free base diastereoisomers (18*a*,**e**) are similar in geometry to their respective protonated forms (12*a*,**e**) (see Table 4). However, a comparison of the energies for the two epimers shows a reversal in their relative stabilities. The axial *N*-methyl free amine (18*a*) is now calculated to be 0.6 kcal mol<sup>-1</sup> more stable than the equatorial epimer, while the equatorial *N*-methyl protonated amine is 0.5 kcal mol<sup>-1</sup> more stable than its epimer. In both cases, these relative energy differences are quite small. As noted above, both 2*a*- and 2*e*-methylcyclo-octane in the boat-chair conformation (4) have been calculated by Hendrickson<sup>23</sup> to be each 0.5 kcal mol<sup>-1</sup> higher in strain energy compared with the unsubstituted cyclo-octane parent structure. The stereochemistry of the methyl entity in these two boat-chair 2-methylcyclo-octane diastereoisomers is similar to that for (12*a*,**e**) and (18*a*,**e**), since the methyl groups in all cases are located on the same site [corresponding to position 2 in (4)] within the staggered 'boat' region of their respective molecules. When viewed as a whole, all these equatorial-axial comparisons show that there is not a major difference in stability for a methyl substituent located in either of the two diastereotopic sites at position 2.

**Comparison of Crystalline versus Calculated Nefopam Hydrochloride Molecular Geometry.**—A comparison between the bonding parameters (*i.e.* bond lengths, bond angles, and torsion angles) of the two crystalline enantiomers [(+)-(1*e*)·H<sub>2</sub>O and (-)-(1*e*)·H<sub>2</sub>O]<sup>14</sup> and between the two reported racemic modifications (±)-(1*e*)<sup>1,15</sup> shows each set to be essentially the same. Perusal of the bonding parameters shows that either of the (±)-(1*e*) or (+)-(1*e*)·H<sub>2</sub>O molecular geometries are more similar to that of calculated (12*e*) than (±)-(1*e*) is to (+)-

(1*e*)·H<sub>2</sub>O. In (12*e*) the pitch or twist of the phenyl ring *vis-à-vis* the benzo moiety is intermediate between that observed in (±)-(1*e*) and (+)-(1*e*)·H<sub>2</sub>O (see Figure 4)].

The (±)-(1*e*) and (+)-(1*e*)·H<sub>2</sub>O crystalline-state structures both show no unusual bond lengths. In all three structures, (±)-(1*e*); (+)-(1*e*)·H<sub>2</sub>O; and calculated (12*e*), the endocyclic angles in the octagonal ring at the junction with the benzo ring were the largest [C(1)–C(11)–C(12): 126.2(1), 125.7(2), 127.5°, respectively; and C(6)–C(12)–C(11): 124.4(2), 123.4(2), 123.7°, respectively]. These larger C–C–C values around the *sp*<sup>2</sup>-hybridized C(11) and C(12) atoms are assumed to result from strain at the junction between the two ring systems. The smallest angle in all three structures was O(2)–C(1)–C(14) [105.6(1), 105.2(2), 107.8°, respectively]. All other angles in the three structures were not unusual, and no significant deviations from aromatic planarity were noted.

Peripheral and transannular non-bonding steric interactions are noted in both crystalline and calculated structures (12*a*,**e**). The boat-(flattened chair) structures (±)-(1*e*); (+)-(1*e*)·H<sub>2</sub>O; and calculated (12*a*,**e**) all suffer from three principal transannular interactions: O(2)···H(61), O(2)···C(6), and C(4)···C(12). The O(2)···H(61) and O(2)···C(6) close contacts are considerably more severe in crystalline (±)-(1*e*) and (+)-(1*e*)·H<sub>2</sub>O than in calculated (12*e*) {*r*[O(2)···H(61)]: 2.32(2), 2.35(1), 2.392 Å, respectively; and *r*[O(2)···C(6)]: 2.766(2), 2.742(3), 2.845 Å, respectively}. On the other hand, the C(4)···C(12) close contact is less severe in the (±)-(1*e*) crystalline state than in calculated (12*e*) [2.953(3) *versus* 2.911 Å, respectively], while it is the same for both crystalline (+)-(1*e*)·H<sub>2</sub>O and calculated (12*e*) [2.914(4) *versus* 2.911 Å, respectively]. The presence of *exo*-1-phenyl and equatorial *N*-methyl substituents on the minimized energy boat-(flattened chair) skeleton (12*e*) affords no significant non-bonded interactions (*E* > 0.6 kcal mol<sup>-1</sup>) other than the three principal transannular interactions noted above.

EFF calculations on the calculated *exo*-phenyl boat-(flattened chair) structures (12*a*,**e**) show that epimerization of the *N*-methyl group from an equatorial to an axial orientation results in a 1,3-*cis*-diaxial interaction between N-CH<sub>3</sub> and H(31), see (19). Reduction of the O(2)–C(3)–C(4)–N(5) torsion angle from 59.8 to 53.4° [in (12*e* and **a**), respectively] reduces this interaction. Using the method of Lambert<sup>30</sup> this angle in solution has been estimated to be 57.5(±1.9) and 52.9(±1.5)° for (1*e*,**a**), respectively.<sup>1</sup>

The molecular structures of *exo*-phenyl boat-(flattened chair) calculated (12*e* and **a**) differ in the orientation of the *N*-methyl group, and correspond to the stereochemistry of the minor and major *N*-protonated solution species, respectively, upon dissolution of crystalline (±)-(1*e*) or (+)-(1*e*)·H<sub>2</sub>O in dichloromethane. It is at present unclear why the axial *N*-methyl group nefopam·HCl species is slightly favoured over the equatorial *N*-methyl group species in dichloromethane solution while both species are present in approximately equal quantities in acidic aqueous media.\*

## Experimental

**Crystallography.**—Dissolution of the racemic modification<sup>2</sup> and the (+)-enantiomer monohydrate<sup>9</sup> of nefopam hydrochloride in dichloromethane and [<sup>2</sup>H]dichloromethane, respectively, followed by slow evaporation yielded the corresponding (±)-(1*e*) and (+)-(1*e*)·H<sub>2</sub>O single crystals as clear, crystalline prisms: (+)-(1*e*)·H<sub>2</sub>O: [α]<sub>D</sub><sup>22</sup> +120° (*c* 1, Me<sub>2</sub>SO) {lit.,<sup>9</sup> (+)- and (-)-(1*e*)·H<sub>2</sub>O, [α]<sub>D</sub><sup>22</sup> +124 and -120.5°

\* A more complete account of the n.m.r. details will be published elsewhere.

(Me<sub>2</sub>SO)} {lit.,<sup>14</sup> (-)-(1e)·H<sub>2</sub>O: [α]<sub>D</sub><sup>22</sup> - 119° (c 1, Me<sub>2</sub>SO)}. Crystals from the solution of the racemic modification (±)-(1e) belonged to the monoclinic system *P*<sub>2</sub><sub>1</sub>/*c*, whereas crystals from the solution of the (+)-enantiomer monohydrate belonged to the orthorhombic system *P*<sub>2</sub><sub>1</sub>2<sub>1</sub>2<sub>1</sub>.

Intensity data were collected at 298 K on an Enraf-Nonius CAD-4 automatic diffractometer. Table 1 provides crystallographic and data collection details. The standard CAD-4 centring, indexing, and data collection programs were used. The unit-cell dimensions were obtained by a least-squares fit of 24 centred reflections in the range of 10° ≤ θ ≤ 15°. Reflections were first measured with a scan of 4.12° min<sup>-1</sup>. The rate for the final scan was calculated from the preliminary scan results so that the ratio *F*/σ(*F*) would be at least 40, and the maximum scan time would not exceed 60 s. If in a preliminary scan *F*/σ(*F*) < 2, this measurement was used as the datum. The first and the last 16 steps of the 96 steps of the scan were considered to be background. During data collection, the intensities of three standard reflections were monitored after every hour of X-ray exposure. No decay was observed in either crystal. In addition, three orientation standards were checked after every 100 reflections to check the effects of crystal movement. If the standard deviation of the *h*, *k*, and *l* values of any orientation reflection exceeded 0.08, a new orientation matrix was calculated on the basis of the recentring of the 24 reference reflections.

The structure of compound (±)-(1e) was solved using MULTAN-78<sup>31</sup> and refined by full-matrix least-squares (SHELX-76).<sup>32,\*</sup> Hydrogen positions were located in a difference Fourier map. The final refinement included anisotropic thermal parameters for the non-hydrogen atoms, and isotropic thermal parameters for the hydrogen atoms. At convergence the final discrepancy indices on *F* were *R*(*F*) = 0.0336 and *R*<sub>w</sub> = 0.0452 for the 2395 reflections with *F*<sub>0</sub><sup>2</sup> ≥ 2σ(*F*<sub>0</sub><sup>2</sup>) and 261 variables.† The residual electron density in the final map was < 0.25 e Å<sup>-3</sup>, and the maximum shift/e.s.d. was 0.003.

Structure (+)-(1e)·H<sub>2</sub>O was solved using the method cited above. The final refinement paralleled that of (±)-(1e), except that hydrogen atoms were refined using the riding model method, and their isotropic thermal parameters were fixed at *U*<sub>iso</sub> = 0.05 Å<sup>2</sup>. The determination of the enantiomer was made by utilizing two separate configurational models: the (1*S*,5*S*)-enantiomer refined to values of *R*(*F*) = 0.0432 and *R*<sub>w</sub> = 0.0690; the (1*R*,5*R*)-enantiomer, obtained by reversing the signs of all atomic co-ordinates, refined to values of *R*(*F*) = 0.0442 and *R*<sub>w</sub> = 0.0700 for the 1844 reflections with *F*<sub>0</sub><sup>2</sup> ≥ 2σ(*F*<sub>0</sub><sup>2</sup>) and 190 variables. A comparison of these residuals indicates that the (1*S*,5*S*)-molecule is the correct enantiomer. Another crystal of (+)-nefopam hydrochloride monohydrate was measured with Cu-K<sub>α</sub> (λ = 1.54178 Å) radiation. Results are *R*(*F*) = 0.0477 and *R*<sub>w</sub> = 0.0799 (1*S*,5*S*), *R*(*F*) = 0.0595 and *R*<sub>w</sub> = 0.0992 (1*R*,5*R*) for 1347 reflections with *F*<sub>0</sub><sup>2</sup> ≥ 2σ(*F*<sub>0</sub><sup>2</sup>) and 190 variables. The residual electron density in the final map was < 0.33 e Å<sup>-3</sup>, and the maximum shift/e.s.d. was 0.007.

The atomic co-ordinates for (±)-(1e) and (+)-(1e)·H<sub>2</sub>O have been deposited with the Cambridge Crystallographic Data Centre.

**Molecular Mechanics Calculations.**—The empirical force field calculations reported here have been performed using the

MOLMEC program developed by Oie *et al.*<sup>25</sup> MOLMEC is a molecular mechanics program which calculates potential energies using a seven-term energy expression (*E* = *E*<sub>b</sub> + *E*<sub>ang</sub> + *E*<sub>tor</sub> + *E*<sub>pl</sub> + *E*<sub>nb</sub> + *E*<sub>hb</sub> + *E*<sub>ei</sub>). These seven terms have the following definitions: *E*<sub>b</sub>, *E*<sub>ang</sub>, and *E*<sub>tor</sub> calculate the deformation due to bond stretching, angle, and torsional deformation, respectively. *E*<sub>pl</sub> calculates the out-of-plane deformation for *sp*<sup>2</sup>-hybridized sites. *E*<sub>nb</sub> corresponds to the interaction energy of atoms which are not bonded to each other, and which are separated by more than two bonds. *E*<sub>hb</sub> describes attractive interaction due to hydrogen bonding, and *E*<sub>ei</sub> calculates Coulomb interaction between atoms which carry partial charges. The analytical expressions for the seven terms, and a description of the derived potential parameters, can be found in ref. 25. The geometry optimizations were carried out using the pattern-search method.<sup>25</sup> The geometries reported here were optimized in regard to all internal variables, *i.e.* bond lengths, bond angles, and torsion angles. In each case, after initial geometry optimisation, the O(2)–C(1)–C(14)–C(15) pitch torsion angle for the phenyl ring was varied by 10° intervals to verify that an energy minimum had indeed been obtained. The optimizations were considered to be converged when (i) the energy of two subsequent iterations differed by less than 5 × 10<sup>-5</sup> kcal mol<sup>-1</sup>, and (ii) no single bond length, bond angle, or torsion angle changed by more than 2 × 10<sup>-4</sup> Å, 5 × 10<sup>-6</sup> and 5 × 10<sup>-5</sup>°, respectively. The partial atomic charges [which are necessary to determine the electrostatic energy (*E*<sub>ei</sub>) in the seven-term formula] were taken from MNDO<sup>34</sup> calculations, using MOLMEC-optimized geometries without the charge term. The differences in energies and geometries by including coulomb interactions were found to be very small.

### Acknowledgements

We thank Dr. R. M. Lain, SRI International, for hospitality to R. G.

### References

- 1 Preliminary report, R. Glaser, S. Cohen, D. Donnell, and I. Agranat, *J. Pharm. Sci.*, 1986, **75**, 772.
- 2 M. W. Klohs, M. D. Draper, F. J. Petracek, K. H. Ginzel, and O. N. Ré, *Arzneim. Forsch. (Drug Res.)*, 1972, **22**, 132.
- 3 R. C. Heel, R. N. Brogden, G. E. Pakes, T. M. Speight, and G. S. Avery, *Drugs*, 1980, **19**, 249.
- 4 (a) K. Hole, O. B. Fasmer, and O. G. Berge, *Pain*, 1984, *Supplement 2*, S231; (b) O. B. Fasmer, O. G. Berge, H. A. Jorgensen, and K. Hole, *J. Pharm. Pharmacol.*, 1987, **39**, 508; (c) S. Hunskaar, O. B. Fasmer, O. J. Broch, and K. Hole, *Eur. J. Pharmacol.*, 1987, **138**, 77.
- 5 N. J. Tresnak-Rustad and M. E. Wood, *Biochem. Pharmacol.*, 1981, **30**, 2847.
- 6 'The Merck Index,' ed. M. Windholz, Merck, Rahway, 10th edn., 1983 p. 484, and references therein.
- 7 Ref. 6, p. 986, and references therein.
- 8 J. R. Bianchine, in 'The Pharmacological Basis of Therapeutics,' eds. L. S. Goodman, A. Gilman, T. W. Rall, and F. Murad, Macmillan, New York, 1985, 7th edn., pp. 485, 489.
- 9 A. G. Bolt, G. Graham, and P. Wilson, *Xenobiotica*, 1974, **4**, 355.
- 10 O. Lingjaerde, personal communication.
- 11 D. F. Smith, *Neurosci. Biobehav. Rev.*, 1986, **10**, 37.
- 12 K. Mislow and J. Siegel, *J. Am. Chem. Soc.*, 1984, **106**, 3319.
- 13 R. Glaser, Q. J. Peng, and A. S. Perlin, *J. Org. Chem.*, 1988, **53**, 2172.
- 14 L. K. Hansen, A. Hordvik, and A. J. Aasen, *Acta Chem. Scand.*, 1984, **38**, 327.
- 15 P. Klüfers, von A. Petersenn, and E. Röder, *Arch. Pharm.*, 1986, **319**, 583.
- 16 J. E. Anderson, E. D. Glazer, D. L. Griffith, R. Knorr, and J. D. Roberts, *J. Am. Chem. Soc.*, 1969, **91**, 1386.
- 17 A. L. Anet, in 'Topics in Current Chemistry,' ed. F. Boschke, Springer-Verlag, Berlin, 1974, vol. 45, pp. 169–220.

\* The atomic scattering factors used in SHELX-76 are taken from ref. 33.

† The final discrepancy index *R*(*F*) is defined as:  $R(F) = (\sum_j |F_{obs,i} - |F_{calc,i}||) / (\sum_j F_{obs,i})$ . The weighted value *R*<sub>w</sub> is defined as  $R_w = \text{SQRT}[\sum_j w_i (|F_{obs,i} - |F_{calc,i}||)^2] / (\sum_i w_i (|F_{obs,i}|)^2)$ , and the particular weighting factor *w*<sub>*i*</sub> used is given in Table 1.

- 18 T. G. Cochran and J. E. Abola, *Acta Crystallogr.*, 1975, **B31**, 919.
- 19 L. Gylbert, *Acta Crystallogr.*, 1973, **B29**, 1630.
- 20 L. M. Trefonas and R. Majeste, *Tetrahedron*, 1963, **19**, 929.
- 21 B. Crammer, Z. Goldschmidt, R. Ikan, and S. Cohen, *J. Chem. Soc., Perkin Trans. 1*, 1984, 887.
- 22 W. E. Oberhänsli, *Cryst. Struct. Commun.*, 1974, **3**, 47.
- 23 J. B. Hendrickson, *J. Am. Chem. Soc.*, 1967, **89**, 7043.
- 24 J. B. Bremner, E. J. Browne, P. E. Davies, C. L. Raston, and A. H. White, *Aust. J. Chem.*, 1980, **33**, 1323.
- 25 T. Oie, G. M. Maggiora, R. E. Christoffersen, and D. J. Duchamp, *Int. J. Quant. Chem., Quant. Biol. Symp.*, 1981, **8**, 1.
- 26 (a) J. A. Glasel, *Biochem. Biophys. Res. Commun.*, 1981, **102**, 703; (b) J. A. Glasel and H. W. Reiher, *Magn. Reson. Chem.*, 1985, **23**, 236.
- 27 C. E. Brown, S. C. Roerig, J. M. Fujimoto, and V. T. Burger, *J. Chem. Soc., Chem. Commun.*, 1983, 1506.
- 28 E. L. Eliel, S. Morris-Natschke, and V. M. Kolb, *Org. Magn. Reson.*, 1984, **22**, 258.
- 29 G. L. Closs, *J. Am. Chem. Soc.*, 1959, **81**, 5456.
- 30 J. B. Lambert, *Acc. Chem. Res.*, 1971, **4**, 87.
- 31 P. Main, S. E. Hull, L. Lessinger, G. Germain, J. P. Declercq, and M. M. Woolfson, 'MULTAN-78: A System of Computer Programmes for the Automatic Solution of Crystal Structures from X-Ray Diffraction Data'; Universities of York and Louvain, 1978.
- 32 G. M. Sheldrick, 'SHELX-76. A Program for Crystal Structure Determination,' University Chemical Laboratory, Cambridge, 1976.
- 33 (a) D. T. Cromer and J. B. Mann, *Acta Crystallogr.*, 1968, **A24**, 321; (b) D. T. Cromer and D. Liberman, *J. Chem. Phys.*, 1970, **53**, 1891.
- 34 M. J. S. Dewar and W. Thiel, *J. Am. Chem. Soc.*, 1977, **99**, 4899, 4906.

Received 2nd July 1987; Paper 7/1176